Phosphorus-31 Nuclear Magnetic Resonance of Highly Oriented DNA Fibers. 2. Molecular Motions in Hydrated DNA†

Toshimichi Fujiwara‡ and Heisaburo Shindo*,§

Tokyo College of Pharmacy, Hachioji, Tokyo 192-03, Japan, and Institute for Protein Research, Osaka University, Suita 565, Japan

Received June 18, 1984

ABSTRACT: ^{31}P nuclear magnetic resonances (NMR) of salmon sperm DNA, poly(rA)·poly(rU), and poly(rA)·poly(dT) fibers were measured as a function of relative humidity. The results indicated that the spectra were strongly perturbed by the molecular motions occurring in the hydrated fibers. The humidity dependence of the spectra at a number of orientations of the fibers relative to the magnetic field was reasonably explained by taking into account at least three motional modes, namely, conformational fluctuations, restricted rotation about a tilted axis, and rotational diffusion about the helical axis. The rotational diffusion about the helical axis was found to perturb the spectral line shapes most strongly, and its constants were 1.5×10^4 and 5.0×10^4 s^{-1} for DNA fibers at 92% and 98% relative humidities, respectively. A DNA–RNA hybrid, poly(rA)·poly(dT), has been shown to adopt different conformations on two strands at a high relative humidity [Zimmerman, S. B., & Pheiffer, B. H. (1981) *Proc. Natl. Acad. Sci. U.S.A. 78*, 78–82], which was unquestionably confirmed in the present study: that is, the ^{31}P NMR spectra from the hydrated form of this polymer were clearly explained by assuming that one strand had an A-like conformation and the other a B-like conformation.

The state of DNA in living things is very complicated: the conformation of the complexes of DNA with proteins and the tremendous condensation of DNA in the cell. The technique of high-resolution ^{31}P nuclear magnetic resonance (NMR)[1] in solids, by which chemical shielding anisotropy can be observed, has been shown to be a unique means to investigate such complex systems of DNA in vivo and in vitro as viruses (Akutsu et al., 1980; DiVerdi & Opella, 1981a; Cross et al., 1983), chromatin (DiVerdi et al., 1981b), powder samples of hydrated DNA (Opella et al., 1981; DiVerdi & Opella, 1981b), and oriented DNA fibers (Shindo et al., 1980, 1981; Shindo & Zimmerman, 1980; Nall et al., 1981). However, the detailed motions of DNA in these complex systems are not well-known.

There are still some controversies on the molecular motions of DNA even in simpler systems such as hydrated DNA samples. DiVerdi & Opella (1981b) have reported the solid-state ^{31}P and ^{2}H NMR studies on DNA powder samples, concluding that neither significant rapid internal motion on the order of a few nanoseconds nor rotational motion about the helical axis occurred in the B-form DNA under their experimental conditions. On the other hand, the rapid internal motion, which is often referred to as conformational fluctuation, has been proposed by many investigators on the basis of a large amount of NMR relaxation data on DNA in solution [see the review of James (1984), and references therein]. Furthermore, the rotational motion has been suggested by us on the basis of the ^{31}P NMR study on oriented DNA fibers at high relative humidities (Shindo et al., 1980). Subsequently, we have shown from the ^{31}P NMR studies that both internal and rotational motions of the double helices simultaneously occur in highly hydrated DNA fibers (Shindo et al., 1983). Generally speaking, in solids, the motion requiring less volume changes by activation is expected to be more predominant; this is an a priori reason why conformational fluctuation and rotational diffusion may be most probable motions occurring in oriented DNA fibers under hydrated conditions.

As described in the preceding paper (Shindo et al., 1985), we had difficulty in determining the phsophodiester orientation from ^{31}P NMR spectra of hydrated DNA fibers, for the spectra were strongly perturbed by the molecular motions of DNA. Since the ^{31}P chemical shielding anisotropy of the phosphodiester is about 190 ppm which corresponds to 15 kHz at a frequency of 80 MHz for ^{31}P nucleus, its spectrum would be most sensitive to the motions of a rate of about 10^4 s^{-1}. Therefore, we realized that the structure of the hydrated form of DNA, i.e., generally the B-form DNA, could not be determined without consideration of the molecular motions in hydrated DNA fibers.

For studying dynamics of DNA there are some advantages in using oriented DNA fibers instead of powder samples or DNA in solution. Main advantages are the following: direct information on the anisotropic motions can be obtained; the amplitude and rate of the motions can be controlled by relative humidity; various forms of DNA or RNA with defined conformations are available. In the present study, we quantitatively evaluate the molecular motions of DNA by means of the line-shape analysis of the ^{31}P NMR spectra from oriented DNA fibers. It is also shown that the models we proposed here can consistently interpret the humidity dependence of the spectral line shapes observed for a variety of polynucleotide fibers.

Theory

The general procedures for calculating the chemical shift spectra of randomly oriented samples undergoing molecular motions have been discussed in Mehring (1983). We will apply these methods to the simulation of the spectra for oriented DNA fibers.

† Supported by a Grant-in-Aid for Scientific Research (56470132).

‡ Institute for Protein Research.

§ Tokyo College of Pharmacy.

[1] Abbreviations: NMR, nuclear magnetic resonance; DNA, deoxyribonucleic acid; RNA, ribonucleic acid; RH, relative humidity.

0006-2960/85/0424-0896$01.50/0

When perfect alignments of the molecules along the fiber axis are assumed, the observed chemical shift $\sigma^{obsd}(\phi,\alpha)$ is given by

$$\rho_{20}^{lab} = \sqrt{\frac{3}{2}}\left(\sigma^{obsd} - \frac{1}{3}Tr\sigma_{ii}\right)$$

$$\rho_{20}^{lab} = \sum_{m,n} D_{m0}^{(2)}(0,\phi,0) D_{nm}^{(2)}(\alpha,\beta,\gamma)\rho_{2n} \quad (1)$$

for the immobilized molecules in oriented samples. σ_{ii} values are the principal chemical shielding tensors, ρ_{2n} is the spherial irreducible shielding tensor in the principal axis system, and $D_{mn}^{(2)}(\Omega)$ represents the Wigner rotation metrices of the second rank. $\Omega = (\alpha,\beta,\gamma)$ represents the Euler angles for the coordinate transformations as defined in Figure 1 in the preceding paper (Shindo et al., 1985), and ϕ is the goniometer angle. Chemical shift spectrum is then given by

$$I(\sigma^{obsd}) = \left|\frac{\delta\alpha}{\delta\sigma^{obsd}}\right| \quad (2)$$

where $|\delta\alpha/\delta\sigma^{obsd}|$ is proportional to the number of the increment $\delta\alpha$ of α which lies in the small range $\delta\sigma^{obsd}$ of σ^{obsd}. Expanding eq 1 and rearranging it, we have the following equation as a function of ϕ and α (Nall et al., 1981)

$$\sigma^{obsd}(\phi,\alpha) = A\sin^2\phi\cos(2\alpha - a) + B\sin 2\phi\cos(\alpha - b) + c \quad (3)$$

where A, B, a, and b are the constants which only depend on β, γ, and σ_{ii}.

The parallel spectrum is simply given by substituting 0° for ϕ in eq 3, leading σ^{obsd} to a constant value C; this means that the parallel spectrum is independent of α and hence unaffected by any rotational motions about the helical axis. The perpendicular spectrum is expressed only by the first angular-dependent term in eq 3 since the second term is zero when ϕ = 90°. Thus, we have the spectral intensity distribution as

$$I(\sigma^{obsd}) = \left|\frac{\delta\alpha}{\delta\sigma^{obsd}}\right|$$

$$I(\sigma^{obsd}) = \frac{1}{2\sqrt{A^2 - (\sigma^{obsd} - C)^2}} \quad (4)$$

for the perpendicular spectrum. Equation 4 gives a symmetric doublet.

Molecular motions in hydrated DNA fibers may be represented mainly by two modes, conformational fluctuations and rotations about certain axes. What we need for the simulation of chemical shift spectra is to evaluate a time average of the chemical shift $\sigma(\phi,\alpha)$ in the presence of such molecular motions. For example, consider a rotational motion about the helical axis, which means the averaging of eq 3 over a certain range of α. It is easy to see from eq 3 that the perpendicular spectrum (ϕ = 90°) is completely averaged out by the rotational motion over ±90° for α, while the 45° spectrum (ϕ = 45°) requires a wider range of ±180° to be averaged. Furthermore, it is easy to show that the 45° spectrum becomes a symmetric doublet when the rotation occurs over ±90° for α.

Conformational Fluctuations. As stated in the preceding paper (Shindo et al, 1985), the broad line width of the parallel spectrum arises from the conformational heterogeneity in the B-form DNA. Since the parallel spectrum is not affected by rotational motion about the helical axis, the narrowing of its spectral line width with the increase in humidity indicates the occurrence of conformational fluctuations.

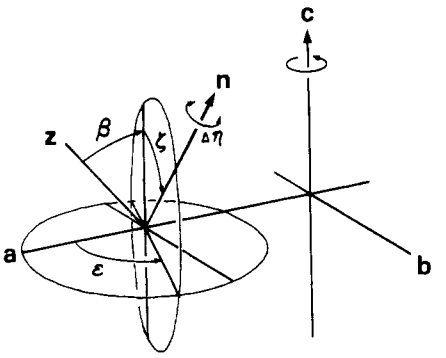

FIGURE 1: Coordinate systems for representing rotational motion about the helical axis c and restricted rotational motion about the tilted axis n. Axis z represents the pricipal axis of the chemical shielding tensor.

For simplicity, let us assume an N-site jump model for the conformational fluctuations of the phosphodiester. The corresponding Euler angles may be denoted as $(\alpha + \alpha_k, \beta_k, \gamma_k)$ for the kth site and a particular α. In case no fluctuations occur, the chemical shift spectrum is rewritten as

$$I(\sigma^{obsd}) = \sum_{k=1}^{N} p_k \left|\frac{\delta\alpha}{\delta\sigma_k}\right|_{\sigma_k=\sigma^{obsd}} \quad (5)$$

where p_k represents the equilibrium population of the phosphodiester in the kth site. In case rapid fluctuations occur among N sites, then the averaged chemical shift and its spectrum are given by

$$\overline{\sigma(\phi,\alpha)} = \frac{\sum_{k=1}^{N} p_k\sigma_k}{\sum_{k=1}^{N} p_k} \quad (6)$$

$$\langle I(\sigma^{obsd})\rangle = \left|\frac{\delta\alpha}{\delta\bar{\sigma}}\right|_{\bar{\sigma}=\sigma^{obsd}} \quad (7)$$

Equation 5 is essentially identical with eq 2, except for the fact that it comprises conformational heterogeneity. In view of the similar formulism between eq 5 and eq 7, both equations should give similar spectral patterns, but the latter generally yields a narrower spectral span and sharper peaks than does the former.

Rotational Motions. Several rotational modes such as restricted rotation, free rotational diffusion, and rotational jump models can be considered. However, the last model is unlikely for polymers in solids. Thus, only the former two models are considered here.

Restricted Rotational Model. Assume that the motion is a rotational motion about a certain axis and that it is sufficiently rapid but that its rotation amplitude is limited within a defined angle range about its axis. Consider that the rotating axis is tilted by an angle ζ with respect to the helical axis system (a, b, c) as shown in Figure 1. Then additional coordinate transformations must be included in eq 1, for example, transformations from the molecular (helical) axis system to the tilted axis system and those from the tilted axis system back to the molecular system. Thus, we have the following equation instead of eq 1:

$$\rho_{20}^{lab} = \sum_{m,n,p,q,r} D_{rn}^{(2)}(0,\phi,0)\, D_{qr}^{(2)}(0,-\zeta,-\epsilon)\, D_{pq}^{(2)}(\eta,0,0)\, D_{mp}^{(2)}(\epsilon,\zeta,0)\, D_{nm}^{(2)}(\alpha,\beta,\gamma)\rho_{2n} \quad (8)$$

Consider that the rotation is free about the tilted axis only within a defined range $-\Delta\eta/2 < \eta < \Delta\eta/2$. The effect of this restricted rotation is equivalent to the arithmetric mean of ρ_{20}^{lab} in eq 8 over this angle range.

If Euler angles ϵ and ζ are 90° and 60°, respectively, the rotating axis is identical with the direction of the backbone chain. In other words, the angle 30° (=90° − ζ) corresponds to the pitch angle of the B-form DNA (Langridge et al., 1960). If ζ is zero, the motion is equivalent to the rotation about the helical axis (see Figure 1).

Of course, the rotational amplitude, $\Delta\eta$, is not necessarily the same for all the phosphodiesters, and it generally has a distribution which may be of a Gaussian type. In this restricted rotational model the parameters to be determined in the simulation of spectra are the tilt angle ζ, the rotation amplitude $\Delta\eta$, and its standard deviation width $\langle\Delta\eta\rangle$.

Free Rotational Diffusion. The general treatments of the diffusional motions have been discussed by Freed et al. (1971) and Meirovitch et al. (1982). We will apply their theories to the line-shape analysis of the ^{31}P NMR spectra from oriented DNA fibers.

When $\langle I_x(t,\Omega)\rangle$ is denoted as the expectation value of the transverse magnetization, spectral intensity $I(\omega)$ is defined as

$$I(\omega) = \int_0^\infty e^{-i\omega t}\int_\Omega \langle I_x(t,\Omega)\rangle p_{eq}(\Omega)\, d\Omega\, dt \qquad (9)$$

where $p_{eq}(\Omega)$ is the equilibrium probability of the Euler angle Ω. Density matrix $\rho(\Omega,t)$, which is required for calculating $\langle I_x(t,\Omega)\rangle$, obeys the following stochastic Liouville equation

$$\frac{\partial}{\partial t}\rho(\Omega,t) = -i[\hat{H}_0 + \hat{H}_1(\Omega)]\ \rho(\Omega,t) + \Gamma\rho(\Omega,t) \qquad (10)$$

where H_0 and H_1 are the Hamiltonians and the circumflex symbol means the Liouville operator. Γ is the Markov operator. For the spin with $I = {}^1/_2$, the expectation value $\langle I_x(t,\Omega)\rangle$ is expressed as follows:

$$\langle I_x(t,\Omega)\rangle = Re(I_x|\exp[-i[\hat{H}_0 + \hat{H}_1(\Omega)t] + \Gamma t]|I_x + iI_y)$$

$$\langle I_x(t,\Omega)\rangle = Re(I_x|\rho_+(t,\Omega)) \propto Re\langle +|\rho_+(t,\Omega)|-\rangle \qquad (11)$$

where $(|\ \ |)$ and $\langle|\ \ |\rangle$ are the bra and ket vectors in the Liouville and Hilbert spaces, respectively. The definition of ρ_+ is clear in eq 11. Expanding the Fourier Laplace transform of eq 11 in terms of the eigenfunctions $G_m(\Omega)$ of Γ, we have

$$\int_0^\infty Re\langle +|\rho_+|-\rangle e^{-i\omega t}\, dt = \sum_m G_m(\Omega)C_m(\omega) \qquad (12)$$

The coefficients $C_m(\omega)$ obey eq 13 which can be obtained from the Fourier Laplace transform of eq 10. Making use of the orthogonal conditions of the eigenfunctions $G_m(\Omega)$, we have

$$[(\omega - \omega') + i\lambda_{m'}]C_{m'}(\omega) + \sum_m \int_\Omega G_{m'}^*(\Omega)G_m(\Omega)\hat{H}_1(\Omega)C_m(\omega)\, d\Omega = -i\delta_{m'0} \qquad (13)$$

where

$$\omega' = \langle -|H_0|-\rangle - \langle +|H_0|+\rangle$$

and

$$G_0(\Omega) = [p_{eq}(\Omega)]^{1/2}$$

λ_m is the eigenvalue of $G_m(\Omega)$ and the asterisk means the Hermitian complex conjugate. Since $G_0(\Omega)$ is constant for the free diffusion, $Re(C_0(\omega))$ is proportional to the spectral intensity.

Considering the interaction of chemical shielding anisotropy with the static field as a Hamiltonian and the free rotational diffusion as a motion, we have

$$H_1(\Omega) = -\sqrt{\frac{2}{3}}\, I_z \sum_{n,l} D_{l0}^{(2)}(0,\phi,0)\ D_{nl}^{(2)}(\alpha,\beta,\gamma)\rho_{2n} \qquad (14)$$

$$\Gamma = D\frac{\partial^2}{\partial\alpha^2} \qquad (15)$$

where D is the rotational diffusion constant. By use of the $(2j+1)$th order complex matrices **A** and **B** and vectors **C** and **K**, eq 13 is expressed as

$$(\mathbf{A} + \mathbf{B})\mathbf{C} = \mathbf{K} \qquad (16)$$

Here, **A** is the diagonal matrix and has the elements

$$A_{kk} = \omega - \omega' - i[(k-j)^2D + T_2^{-1}]$$

where T_2 is the transverse relaxation time. **B** has the following elements

$$B_{lk} = 0 \qquad (|k-l| > 2)$$

$$B_{lk} = -\sqrt{\frac{2}{3}}\sum_{n=2}^{-2} D_{l-k0}^{(2)}(0,\phi,0)\ D_{nl-k}^{(2)}(0,\beta,\gamma)\rho_{2n} \qquad (|k-l| \le 2)$$

and $K_l = -i\delta_{l0}$ for the elements of **K** and $C_l = C_{l-j-1}(\omega)$ for the elements of **C**. Equation 16 has been solved by using the Gaussian elimination method which is known to be numerically stable. The calculations were stable enough with $j \le 50$ depending on the diffusion constant.

In this free rotational diffusion model, the only parameter to be determined in the spectral simulation is the diffusion constant D. Because of a long computing time for the calculation we did not take into account the distributions of Euler angles β and γ for the phosphodiesters.

Results and Discussion

The ^{31}P NMR spectra from salmon sperm NaDNA, poly(rA)·poly(rU), and poly(rA)·poly(dT) fibers strongly suggested the occurrence of the conformational fluctuations and rotational motions of DNA in the fiber in the humidity range of 87–98% RH. Figure 2 shows the humidity dependence of the chemical shifts and line widths of the parallel and perpendicular spectra of NaDNA fibers. As was discussed in the preceding paper (Shindo et al., 1985), the fiber forms the A-form DNA below 84% RH and the B-form DNA above 87% RH. We are now interested in the B-form DNA. The characteristic features of the spectra of the B-form DNA are as follows: (1) a steep narrowing in line width of the parallel spectra occurs with the increase in humidity (Figure 2); (2) the perpendicular spectrum is a sharp single line but has a longer shoulder on the upfield side at intermediate humidities [see the perpendicular spectra at 87% and 89% RH in Figure 2 in the preceding paper (Shindo et al., 1985)]; (3) the perpendicular spectrum shows an upfield shift with increasing humidity (Figure 2); (4) the spectrum (ϕ = 45°) is a doublet at 92% RH and a bell-shaped pattern at 98% RH [see the 45° spectra in Figure 2 in the preceding paper (Shindo et al., 1985)]; (5) the line width is on the order of $\Delta\nu(45°) > \Delta\nu(0°) \ge \Delta\nu(90°)$ at 92% RH; (6) upon humidity change from 92% to 98% RH, $\Delta\nu(0°)$ remains unchanged, but $\Delta\nu(90°)$ becomes narrower to be half of $\Delta\nu(0°)$, i.e., $\Delta\nu(0°) = 2\Delta\nu(90°)$ at 98% RH. Here, $\Delta\nu(\phi)$ represents the half-height line width at goniometer angle ϕ. On the other hand, the characteristic features for the A′ form of poly(rA)·poly(rU) fibers at high RH are as follows [see the spectra at 98% RH in Figure 5 in the preceding paper (Shindo et al., 1985)]: (7) the 45° spectrum is no longer a doublet but exhibits a strong intensity at the center, and (8) the order of the line widths is $\Delta\nu(90°) > \Delta\nu(45°) > \Delta\nu(0°)$. These essential features (items 1–8) must be interpreted quantitatively in terms of the motional models.

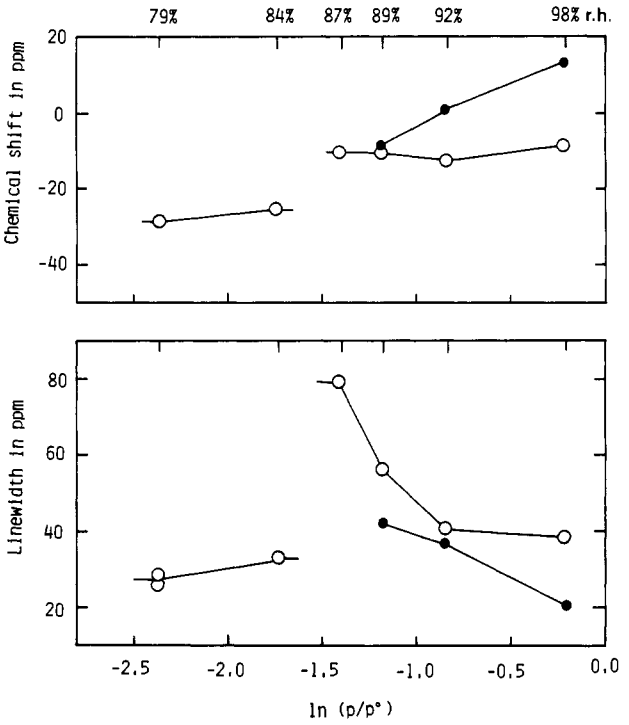

FIGURE 2: Humidity dependence of chemical shifts and line widths of the ^{31}P NMR spectra from salmon sperm NaDNA fibers oriented parallel (○) and perpendicular (●) to the magnetic field. Chemical shifts were measured as upfield positive relative to the external phosphoric acid (85%). Original spectra have been reported in Figure 2 in the preceding paper (Shindo et al., 1985).

Conformational Fluctuations. As we have stated in the previous studies (Shindo et al., 1980, 1984), and also in the preceding paper (Shindo et al., 1985), the broad line width of the parallel spectra arises mainly from the conformational heterogeneity of the B-form DNA. The observed line widths of about 40 and 80 ppm for the parallel spectra at 92% and 87% RH (Figure 2) can easily be attributed to the standard deviations 5° and 11° for $\langle\beta\rangle$, respectively, although the variation in the Euler angle γ resulted in only a small influence on the parallel spectrum. Since the parallel spectrum is not affected by the rotational motion about the helical axis, the narrowing of the parallel spectrum with the increase in humidity is attributed to the narrowing of the conformational distribution, whatever the reason may be. It is most likely that the increasing rate and range of conformational fluctuations with increasing humidity cause effective heterogeneity of the phosphodiesters to be reduced; this gives rise to the line narrowing of the spectrum but makes only small changes in the pattern of the perpendicular spectrum as mentioned under Theory. Therefore, such fluctuations can interpret item 1 but not item 2. Thus, there must exist another motional mode resulting in the asymmetric single line of the perpendicular spectrum.

Restricted Rotation about a Tilted Axis. The conformational fluctuations of the backbone occur as a consequence of torsional motions about the six successive bonds. Therefore, such motions may be approximated to a restricted rotation about the backbone. In a more general case, this rotating axis may be tilted by an angle ζ from the helical axis as described in Figure 1. Figure 3 shows the variations in the spectral line shape as a function of rotational amplitude for two different tilt angles ζ, where Gaussian distributions with standard deviations $\langle\beta\rangle = 5°$ and $\langle\gamma\rangle = 15°$ were assumed for the Euler angles β and γ. With regard to the parallel spectrum, so long as the distributions of the Euler angles are constant, the line

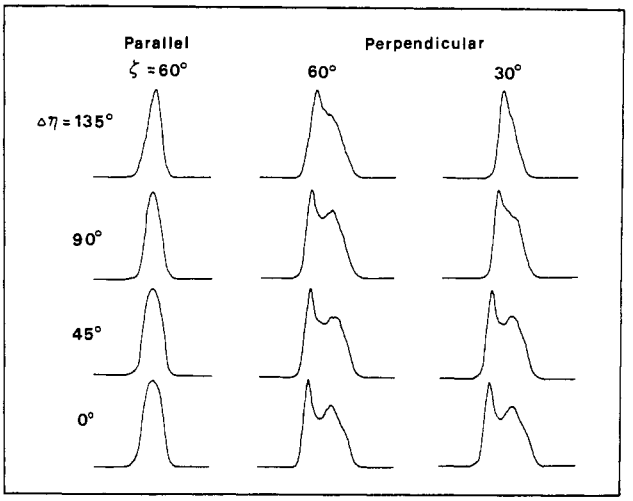

FIGURE 3: Change in line shape of the parallel and perpendicular spectra as a function of the rotational amplitude $\Delta\eta$ for the restricted rotational motion about a particular axis which tilts by ζ from the helical axis when $\epsilon = 90°$.

width is not appreciably influenced by the rotation amplitude $\Delta\eta$, although the line shape is slightly changed to an inversed V shape from a Gaussian type. On the other hand, the distorted doublet pattern of the perpendicular spectrum gradually turns into an asymmetric single line, and its maximum peak position shifts toward upfield with increasing rotation amplitude. The latter result agrees with the observation that the peak position of the perpendicular spectrum shifts upfield with the increase in relative humidity (Figure 2). The spectral line shape under the restricted rotation with an amplitude $\Delta\eta = 135°$ about the tilted axis seems to resemble those observed for the B form of DNA fibers in the humidity range from 87% to 98% RH [perpendicular spectra C and D in Figure 2 in the preceding paper (Shindo et al., 1985)]. An essential feature deduced from the restricted rotation model is that the model predicts the asymmetric single line for the perpendicular spectrum and the upfield shift of its peak with increasing relative humidity. Thus, items 2 and 3 can be qualitatively explained in terms of the rotational motion about a tilted axis. As we shall see later, no large rotational amplitude such as $\Delta\eta = 135°$ may be actually required for this motion because of the presence of another rotational motion about the helical axis.

Rotational Diffusion about the Helical Axis. It appears that the most effective motion to collapse a doublet of the perpendicular spectrum into a single line is the rotational motion about the helical axis. It is indeed possible to consider that DNA molecules can diffuse in the semicrystalline fiber at high relative humidities, in which more than 100% of water by weight is known to be absorbed. However, the lateral diffusion of the whole molecule is highly restricted because of the high activation energy required for such a movement and also because of the parallel alignments of very high molecular weight DNA. Thus, the diffusional rotation is more likely to occur in hydrated fiber. It is interesting, therefore, to know how the spectral pattern is perturbed by the rotation about the helical axis.

B-Form DNA. By use of eq 16, the spectra at three representative goniometer angles 0°, 45°, and 90° were calculated for various sets of Euler angles β and γ. A series of the spectra for a representative case (i.e., Euler angles $\beta = 55°$ and $\gamma = 30°$) are displayed in Figure 4 as a function of number N (in ppm), where the diffusion constant D is given by $D = (2\pi)\,80.7N\ s^{-1}$. Several points can be noted from Figure 4: the

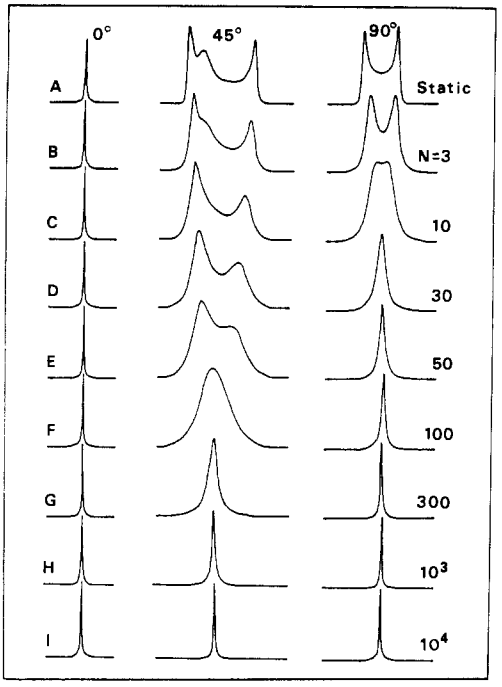

FIGURE 4: Calculated spectra of the B-form DNA fibers at three goniometer angles as a function of diffusion constant for the rotational diffusion about the helical axis. Rotational diffusion constant D is given by $D = (2\pi)80.7N$, where N is repesented in ppm as indicated. The Euler angles of the phosphodiester used for the calculations were 55° and 30° for β and γ, respectively. Distributions of the Euler angles were not taken into account, but a 4 ppm line broadening was made.

parallel spectrum remains unchanged, and the 45° spectrum exhibits a doublet with a disproportional intensity at intermediate diffusion constants but collapses into a singlet at the constants over $N = 100$ ppm, i.e., $D > 5.1 \times 10^4$ s^{-1}. Furthermore, the perpendicular spectrum is always narrower than the 45° spectrum. When the distribution of Euler angles β and γ are taken into account as before, the line width of the parallel spectrum, which fits the observed broad line width, can be obtained, although such calculations would be very time consuming. When the above circumstances are considered, it appears that Figure 4 gives the answer to items 4 and 5, which are concerned with the doublet pattern at the goniometer angle 45° and the relationship of spectral line widths, $\Delta\nu(45°) > \Delta\nu(90°)$. The difference in the dependence of the chemical shift spans on the diffusion constant between the perpendicular and the 45° spectra is rationalized by eq 3; the angle range $\alpha = \pm 90°$ is required to perfectly average the perpendicular spectrum ($\phi = 90°$), whereas the range $\pm 180°$ is necessary to average the 45° spectrum. The unequality between $\Delta\nu(0°)$ and $\Delta\nu(90°)$ depends on the distribution of Euler angles β and γ.

The characteristic feature (item 6) is due to the fact that the rotational motion about the fiber axis does not cause any motional narrowing in the parallel spectrum while it does in the perpendicular spectrum. When the motion is rapid enough, the apparent principal values of the chemical shielding tensor become axially symmetric. In this case the following equation is held:

$$2\left[\sigma^{obsd}(\phi = 90°) - \frac{1}{3}Tr\sigma_{ii}\right] = \sigma^{obsd}(\phi = 0°) - \frac{1}{3}Tr\sigma_{ii}$$

This equation implies that the distribution of Euler angles β and γ would cause the parallel spectrum to broaden twice as much as the perpendicular spectrum. The imperfect alignment of molecules along the fiber axis gives rise to the same effect

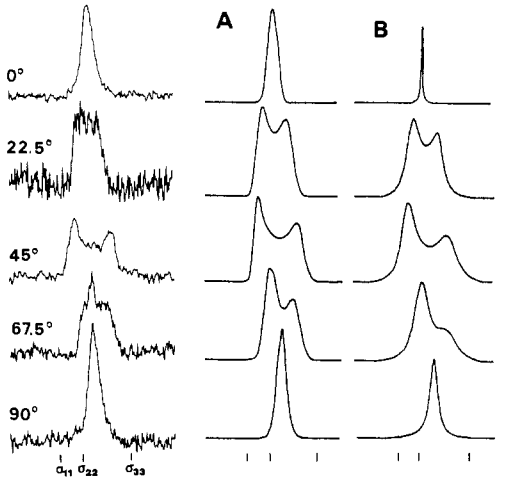

FIGURE 5: Dipolar decoupled ^{31}P NMR spectra (80.7 MHz) of NaDNA fibers at 92% RH at various goniometer angles as indicated. The observed spectra are compared with those simulated on the bases of two models, A and B: model A is the restricted rotation model, and model B is the rotational diffusion model about the helical axis. Parameters used for model A are 130° and 90° for rotational amplitude $\Delta\eta$ and its standard deviation $\langle\Delta\eta\rangle$ from $\Delta\eta$, respectively. Diffusion constant used for model B is $N = 30$ ($D = 1.5 \times 10^4$ s^{-1}).

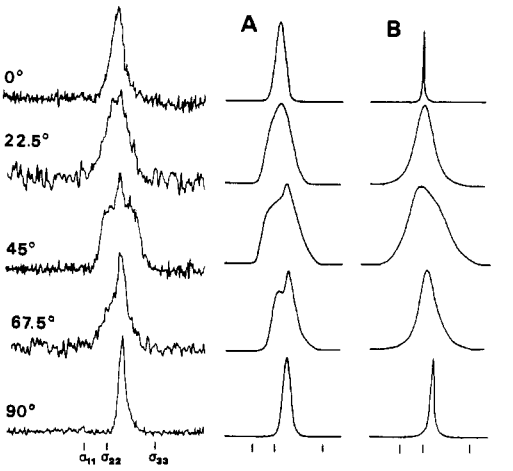

FIGURE 6: Dipolar decoupled ^{31}P NMR spectra (80.7 MHz) of NaDNA fibers at 98% RH at various goniometer angles as indicated. The observed spectra are compared with those calculated from two models, restricted rotation (A) and rotational diffusion (B). Parameters used for model A are 220° and 90° for rotational amplitude $\Delta\eta$ and its standard deviation $\langle\Delta\eta\rangle$ from $\Delta\eta$, respectively. Diffusion constant used for model B is $N = 100$ (i.e., $D = 5.1 \times 10^4$ s^{-1}).

on the line width as the distribution of Euler angles. Thus, the characteristic feature (item 6) is accounted for by the occurrence of the rotational motion about the helical axis. However, it can be seen from Figure 4 that the calculated perpendicular spectra always retain symmetry at any diffusion constant. This is inconsistent with the asymmetric single line in the observed perpendicular spectra; such an asymmetry was explained in terms of the restricted rotation about a tilted axis.

Figures 5 and 6 show a series of the spectra observed for NaDNA fibers at several different goniometer angles at 92% and 98% RH and compare them with the simulated spectra. Two sets of spectra A and B correspond to the two following cases: one is the restricted rotation about the helical axis (A), and the other is the rotational diffusion model (B). The former model is equivalent to the restricted rotation about a tilted axis when the tilted angle $\zeta = 0°$. It is remarkable that these two models show an essentially good agreement both in the line shape and in the peak positions with those of the observed spectra. The parameters used for the rotational diffusion

Table I: Structural Parameters β and γ of the Phosphodiesters and Rotational Diffusion Constants Estimated for the B-Form NaDNA and Poly(rA)·Poly(dT) Fibers at High Relative Humidities

materials	sequences	Euler angles (deg) β	Euler angles (deg) γ	diffusion constant (s^{-1})
salmon sperm NaDNA				
at 92% RH		53 ± 5	30 ± 10	1.5×10^4
at 98% RH		53 ± 5	30 ± 10	5.0×10^4
poly(rA)·poly(dT)				
at 92% RH	rAprA	85 ± 5	50 ± 5	1.0×10^4
	dTpdT	56 ± 5	10 ± 10	

model are listed in Table I. Some discrepancies between the observed and simulated spectra (both A and B) can be seen in the intensity distributions at goniometer angles 45° and 67.5° in Figure 6, suggesting that the models are not fully satisfactory, although it is clear that the rotational motions are most predominant for determining the spectral line shapes. The sharp lines of the parallel spectra in Figure 5 and 6 would be corrected for model B by taking into account the conformational heterogeneity of the phosphodiesters as described before.

Models A and B give indistinguishable spectra. However, model A has more parameters than model B, and moreover, it gives no information about the rate of the motion. The parameters, $\Delta\eta$ for the rotation amplitude and $\langle\Delta\eta\rangle$ for its distribution, were somewhat subjective in simulating the spectra. Thus, it is physically more acceptable that the rotational motion about the helical axis of the double-stranded DNA in the fiber is a diffusion process rather than the restricted rotation within a potential well. As described under Theory, according to the restricted rotation model, the 45° spectrum would always be a doublet when the rotation amplitude reaches ±90°. However, such a doublet was not observed for poly(rA)·poly(rU) fibers at high RH. Thus, we believe that model B is much simpler, describing the realistic situation, whereas model A merely provides a formalism to simulate the observed spectra.

A-Form DNA. By use of a set of Euler angles $\beta = 75°$ and $\gamma = 59°$ for the phosphodiesters of the typical A form of DNA, the spectra were calculated as a function of the diffusion constant and are shown in Figure 7. Remarkably, in contrast to the doublet partterns of the B-form DNA, the 45° spectrum of the A′ form is approximately a single line at the intermediate diffusion constants, N = 20–50 ppm. Therefore, the characteristic features (items 7 and 8) of the ^{31}P spectra from poly(rA)·poly(rU) fibers at 98% RH are self-evident from Figure 7. However, the relationship $\Delta\nu(90°) > \Delta\nu(45°) > \Delta\nu(0°)$ among the line widths observed for this polymer is found to be held only in the range of diffusion constants, N = 0–30 ppm. For the same reason as mentioned previously, since the perpendicular spectrum more strongly depends on the diffusion constant than the 45° spectrum, the line width would be $\Delta\nu(0°) > \Delta\nu(45°) > \Delta\nu(90°)$ when the diffusion constant is sufficiently high.

Poly(rA)·Poly(dT). Finally, it is interesting to simulate the spectra from the poly(rA)·poly(dT) hybrid fibers at high RH. As we discussed in the preceding paper (Shindo et al., 1985), it appears that at high relative humidities the poly(rA) chain has a conformation of the A family and the poly(dT) chain has a conformation of the B family. In view of the structure proposed for this polymer (Zimmerman & Pheiffer, 1981) and of the observed chemical shifts, the most probable Euler angles of the phosphodiesters on the poly(rA) chain were found to be 85° and 50° for β and γ, repectively, and those on the poly(dT) chain were 55° and 10°. By use of these conformational parameters, the spectra from each strand were calculated for various diffusion constants. In Figure 8 the observed spectra at 92% RH are compared with the composite spectra from the two strands at a diffusion constant, N = 20, where the intrinsic line widths of 5 and 15 ppm were assumed for the poly(rA) and poly(dT) strands, respectively. It is clear from Figure 8 that the observed and simulated spectra are in excellent agreement with each other in the line shapes as well as in the peak positions.

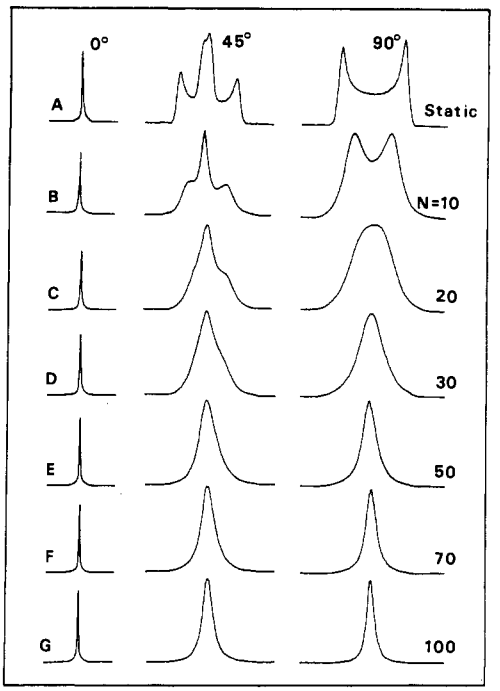

FIGURE 7: Calculated spectra of the A-form DNA fibers as a function of diffusion constant. The Euler angles used are 75° and 59° for β and γ, respectively. See details in the legend of Figure 4.

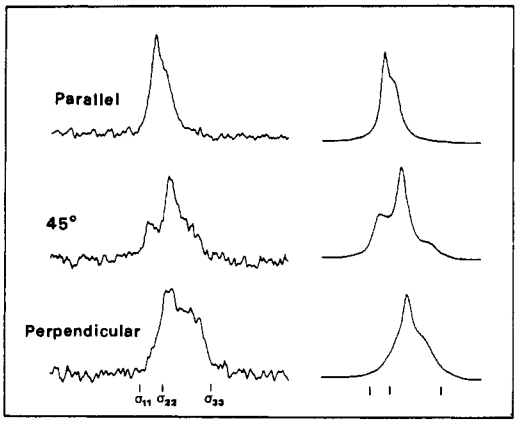

FIGURE 8: Dipolar decoupled ^{31}P NMR spectra (80.7 MHz) of poly(rA)·poly(dT) hybrid fibers at 92% RH at three goniometer angles as indicated. On the basis of a rotational diffusion model, simulated spectra (right) were calculated for the B-like form of this hybrid with different Euler angles, β and γ, of the phosphodiesters on the antiparallel chains. See details in the text.

Molecular Motions in Hydrated DNA Fibers. We demonstrated by the line-shape analysis of the ^{31}P chemical shift spectra of a variety of polynucleotide fibers that the molecular motions of DNA in the fiber can be described by at least three modes: conformational fluctuations, the restricted rotation about a tilted axis, and the rotational diffusion about the helical axis. On the other hand, the molecular motions of DNA in solution may be conveniently classified into three categories:

overall motion, large segmental motions, and internal motion [see the review of James (1984)]. The overall motion may not be permitted in oriented DNA fibers because the DNA molecules of high molecular weight are aligned parallel in the fiber. For the same reason, the large segmental motion which usually characterizes the hydrodynamic properties of DNA in solution may also be restricted in the fiber. In other words, DNA in the fiber is no longer described as a random-flight chain. It has been shown from the ^{31}P relaxation study of hydrated DNA fibers (Shindo et al., 1983) that the internal motion, which is often referred to as conformational fluctuations, occurs in the same manner as in DNA in solution. As stated by James (1984), such conformational fluctuations including the structural fluctuations of the bound water molecules may act in a concerted fashion, entailing alterations in the torsion angles about the backbone bonds and twisting (winding and unwinding motions). Or inversely, such collective motions of Brownian type may transiently cause a strain along the chain, which may usually be released by the local conformational changes without serious damage to the structures such as strand separation. The alterations in the torsion angles along the backbone bonds may be described as the restricted rotation, on the average, about a certain tilted axis (i.e., the backbone chain); such a motion seems to actually occur as manifested in the asymmetry of the perpendicular spectra of the B form of NaDNA fibers at 87% and 89% RH [see spectra C and D in Figure 2 in the preceding paper (Shindo et al., 1985)].

As can be seen in Table I, the diffusion constants for the rotational diffusion about the helical axis were found to be 1.5×10^4 s^{-1} and 5.0×10^4 s^{-1} at 92% and 98% RH, respectively. It is remarkable that the latter value is very close to the value 6.2×10^4 s^{-1} for the rotational motion evaluated from the ^{31}P NMR relaxation data of DNA fibers at 98% RH (Shindo et al., 1983). DiVerdi & Opella (1981b) have reported the ^{31}P and ^2H NMR studies on the randomly oriented B-form DNA, stating that the motions of DNA at the phosphodiester sites are more or less isotropic and that the rotational motion about the helical axis is unlikely. The latter statement is based on the observation that the quadrupolar splitting of the ^2H spectra of the B-form DNA containing a deuterium-labeled thymidine base at position 8 retains its separation even at relatively high temperatures. It should be emphasized, however, that the NMR time scale is quite different between the ^{31}P and ^2H spectra: 15 kHz for the ^{31}P chemical shielding anisotropy at 80 MHz and 200 kHz for the ^2H quatrupolar splitting. As a result, the motion that most effectively perturbs the chemical shift spectrum has only a little effect on the ^2H spectrum; this is exactly relevant to the present case. A strong dependence of the spectral pattern of the goniometer angles (Figures 5 and 6) provides indisputable evidence for the occurrence of rapid rotational diffusion about the helical axis in hydrated DNA fibers.

ACKNOWLEDGMENTS

We thank Drs. H. Akutsu and Y. Kyogoku (Osaka University) for their critical reading of the manuscript and their useful discussions. We also appreciate the staff of Crystallographic Research Center of the Institute for Protein Research in Osaka University for providing us with their computer facilities.

Registry No. Poly(rA)·poly(rU), 24936-38-7; poly(rA)·poly(dT), 27156-07-6.

REFERENCES

Akutsu, H., Satake, H., & Franklin, R. M. (1980) *Biochemistry 19*, 5264–5270.

Cross, T. A., Tsang, P., & Opella, S. J. (1983) *Biochemistry 22*, 721–726.

DiVerdi, J. A., & Opella, S. J. (1981a) *Biochemistry 20*, 280–284.

DiVerdi, J. A., & Opella, S. J. (1981b) *J. Mol. Biol. 149*, 307–311.

DiVerdi, J. A., Opella, S. J., Ma, R.-I., Kallenback, N. R., & Seeman, N. C. (1981) *Biochem. Biophys. Res. Commun. 102*, 885–890.

Freed, J. H., Bruno, G. V., & Polnaszek, C. F. (1971) *J. Phys. Chem. 75*, 3385–3399.

James, T. L. (1984) in *Phosphorus-31 NMR* (Gorenstein, D., Ed.) pp 340–398, Academic Press, New York.

Langridge, R., Wilson, H. R., Hooper, C. W., Wilkins, M. H. F., & Hamilton, L. D. (1960) *J. Mol. Biol. 2*, 19–37.

Mehring, M. (1983) in *Principles of High Resolution NMR in Solids*, 2nd revised and enlarged ed., Springer-Verlag, Berlin, Heidelberg, New York.

Meirovitch, E., Igner, D., Igner, E., Moro, G., & Freed, J. H. (1982) *J. Chem. Phys. 77*, 3915–3938.

Nall, B. T., Rothwell, W. P., Waugh, J. S., & Rupprecht, A. (1981) *Biochemistry 20*, 1881–1887.

Opella, S. J., Wise, W. B., & DiVerdi, J. A. (1981) *Biochemistry 20*, 284–290.

Shindo, H., & Zimmerman, S. B. (1980) *Nature (London) 283*, 690–691.

Shindo, H., Wooten, J. B., Zimmerman, S. B., & Pheiffer, B. H. (1980) *Biochemistry 19*, 518–526.

Shindo, H., Wooten, J. B., & Zimmerman, S. B. (1981) *Biochemistry 20*, 745–750.

Shindo, H., Matsumoto, U., Akutsu, H., & Fujiwara, T. (1983) *Jerusalem Symp. Quant. Chem. Biol. 16*, 169–182.

Shindo, H., Fujiwara, T., Akutsu, H., Matsumoto, U., & Shimidzu, M. (1984) *J. Mol. Biol. 174*, 221–229.

Shindo, H., Fujiwara, T., Akutsu, H., Matsumoto, U., & Kyogoku, Y. (1985) *Biochemistry* (preceding paper in this issue).

Zimmerman, S. B., & Pheiffer, B. H. (1981) *Proc. Natl. Acad. Sci. U.S.A. 78*, 78–82.